International Journal of Coal Science & Technology (2024) 11:37
https://doi.org/10.1007/s40789-024-00672-2

RESEARCH

Synergistic CO_2 mineralization using coal fly ash and red mud as a composite system

Zhenchao Yao[1] · Yugao Wang[1] · Jun Shen[1] · Yanxia Niu[1] · Jiang Feng Yang[1] · Xianyong Wei[2]

Received: 10 September 2023 / Revised: 24 December 2023 / Accepted: 29 February 2024

Abstract
CO_2 mineralization plays a critical role in the storage and utilization of CO_2. Coal fly ash (CFA) and red mud (RM) are widely utilized as CO_2 mineralizers. However, the inert calcium species in CFA limit its carbonation capacity, meanwhile the substantial Ca^{2+} releasing of RM is hindered by a covering layer of calcium carbonate. In this study, CO_2 mineralization in a composite system of CFA and RM was investigated to enhance the carbonation capacity. Multiple analyzers were employed to characterize the raw materials and resulting mineralization products. The results demonstrated that a synergistic effect existed in the composite system of CFA and RM, resulting in improving CO_2 mineralization rate and efficiency. The produced calcium carbonate was ectopically attached the surface of CFA in the composite system, thus slowing down its coverage on the surface of RM. This phenomenon facilitated further releasing Ca^{2+} from the internal RM, thereby enhancing CO_2 mineralization efficiency. Meanwhile, the inclusion of RM significantly improved the alkalinity of the composite system, which not only promoted the dissolution of Ca^{2+} of the inert $CaSO_4(H_2O)_2$ in CFA, but also accelerated CO_2 mineralization rate. The investigation would be beneficial to CO_2 mineralization using industrial solid wastes.

Keywords CO_2 mineralization · Coal fly ash · Red mud · Synergistic effect

1 Introduction

Escalating greenhouse gas emissions, especially CO_2, have inflicted significant harm on global ecosystems, resulting in devastating climate changes. Various strategies have been proposed for the utilization and storage of CO_2, encompassing land filling (Afra et al. 2023), chemical conversion (Fernández-González et al. 2022), biotransformation (Bajracharya et al. 2017) and mineralization (Koytsoumpa et al. 2018). Among these approaches, CO_2 mineralization stands out as an effective and sustainable method for the permanent and safe storage of CO_2 in a stable carbonate mineral form, emulating natural rock weathering processes (Zevenhoven et al. 2008; Seifritz 1990).

✉ Yugao Wang
wangyugao@tyut.edu.cn

[1] School of Chemical Engineering and Technology, Taiyuan University of Technology, Taiyuan, Shanxi 030024, China

[2] Key Laboratory of Coal Processing and Efficient Utilization, Ministry of Education, University of Mining & Technology, 221116 Xuzhou, Jiangsu, China

CO_2 mineralization involves the carbonation of industrial alkali metal wastes and natural minerals (Romanov et al. 2015). The direct reaction between CO_2 and natural minerals is hampered because of needing energy-intensive pretreatment to release their alkaline components (Wang and Maroto-Valer 2011). In contrast, industrial alkali metal wastes like coal fly ash (CFA) and red mud (RM) have gained prominence due to their low cost, high reactivity, and proximity to CO_2 emission sources (Sanna et al. 2012). While CFA exhibits a low Ca^{2+} content and inert nature, limiting its carbonation capacity during CO_2 mineralization. RM has a high Ca^{2+} content, but the Ca^{2+} cannot be quickly and fully released because the resulting calcium carbonate would cover the remained RM, thereby reducing its overall carbonation potential and efficiency. Consequently, there is a pressing need for further advancements to enhance the carbonation capacity of both CFA and RM for CO_2 mineralization.

As a byproduct of coal combustion, CFA accounts for 60 wt%–88 wt% of the total combustion residue of coal-fired power plants (Yao et al. 2015; Ram and Mohanty 2022; Brent et al. 2012). CFA contains various inorganic components such as SiO_2, Al_2O_3, CaO, Fe_2O_3, Na_2O, MgO,

and $CaSO_4$ (Yuan et al. 2022). Despite being used as a filler for bricks, roads, or dams, a significant amount of CFA is still discarded in soil or ash ponds, raising serious environmental concerns (Liu et al., 2018). Exploring the potential of CFA for CO_2 mineralization presents a promising opportunity to permanently and securely store CO_2 in stable carbonate minerals.

Previous studies have primarily focused on the feasibility of CFA carbonation, employing gas-solid and aqueous routes (Pei et al. 2017; He et al. 2013), with the latter being more effective (Noack et al. 2014; Ding et al. 2022; Dananjayan et al. 2016). Ho et al. (2021) employed low-Ca^{2+} containing CFA for direct wet mineralization of CO_2, achieving a maximum carbonation capacity of 31.0% (6.3 g-CO_2/kg-CFA). Yuan et al. (2022) found that CFA exhibited higher carbonation capacity under supercritical CO_2 conditions than that low-pressure conditions, reaching a maximum of 54.9 g-CO_2/kg-CFA. Ji et al. (2017) discovered that CFA containing active Ca/Mg crystal phases exhibited enhanced CO_2 solidification, and the reactivity of calcium phases surpassed that of magnesium phases.

The content and form of Ca^{2+} in CFA play a pivotal role in determining its CO_2 sequestration potential. Highly active calcium crystal phases in CFA include lime (CaO), slaked lime (Ca $(OH)_2$), calcium silicate ($CaSiO_3$), and gypsum ($CaSO_4$). Lime (CaO), slaked lime (Ca $(OH)_2$), and calcium silicate ($CaSiO_3$) can directly participate in the mineralization reaction with CO_2, while the inert gypsum ($CaSO_4$) would generate $CaCO_3$ with CO_2 only in an alkaline environment (Wang et al. 2020). Therefore, during CFA carbonation, the introduction of another alkaline solid waste, such as RM or calcium carbide slag, may be beneficial to the mineralization reaction between $CaSO_4$ in CFA and CO_2 under alkaline conditions. The approach has the potential to significantly enhance the utilization rate of Ca^{2+} in CFA and improve its effectiveness for CO_2 sequestration.

RM is an alkaline solid waste generated during the alumina refining process of bauxite. RM poses significant environmental hazards and incurs high disposal costs (Genç-Fuhrman et al. 2004; Yang and Xiao 2008; Tsakiridis et al. 2004). Due to its high content of alkaline components, such as CaO, RM exhibits potential for CO_2 sequestration through carbonation processes. Mucsi et al. (2021) found that extending the reaction time and performing mechanical grinding increased the carbonation capacity of RM by 1.7%, while significantly reducing the pH of the resulting suspension. Revathy et al. (2021) demonstrated that temperature, CO_2 pressure, liquid-to-solid ratio, and reaction time had a significant impact on the carbonation capacity of RM.

Currently, research efforts primarily focus on utilizing CO_2 absorption to neutralize the alkalinity of RM, with limited attention paid to its carbonation capacity. One of the major challenges associated with RM is its low carbonation capacity and the generation of water-soluble Na_2CO_3. Adding gypsum or concentrated brine could increase the content of free and soluble Ca^{2+} and Mg^{2+} in RM system, thus enhancing its ability to mineralize CO_2 (Han et al. 2017).

Due to the huge output and containing abundant calcium-bearing compounds, CFA and RM are remarkably promising for CO_2 mineralization in a large scale. The combination of CFA and RM holds great promise for enhancing the carbonation capacity for CO_2, given that the strong alkalinity of RM would facilitate releasing inert Ca^{2+} from CFA, and thus reducing the overall alkalinity of RM (Liang et al. 2018). This approach provides a feasible solution for CO_2 sequestration and solid waste management.

In the study, the potential of utilizing CFA and RM as a composite system was investigated to improve the carbonation capacity without other additional chemicals. The impact of the CFA and RM compound system on CO_2 mineralization rate was monitored using a pH meter, while the effect of the compound system on CO_2 mineralization efficiency was determined through thermogravimetry. Additionally, mineral phases, microstructures, and particle distributions of the original samples and the mineralization products were analysed using X-ray diffraction (XRD) and scanning electron microscopy (SEM).

Table 1 Chemical composition of the raw materials (wt%)

Oxide	CFA	RM
SiO_2	45.53	19.39
Al_2O_3	26.94	5.53
Fe_2O_3	10.85	8.60
CaO	3.20	54.32
TiO_2	2.33	-
K_2O	1.94	0.29
SO_3	1.45	0.83
P_2O_5	0.87	0.87
Na_2O	-	2.75
MgO	0.29	0.88

2 Experimental section

2.1 Materials

CFA and RM were collected from a power plant and an alumina plant in Shanxi Province, China, respectively. They were dried at 105 °C for 24 h prior to use. Then, RM was crushed with a pulverizer and passed through 200-mesh sieve. CO_2 used in the experiments had a purity of 99.99%. The chemical composition of the CFA and RM samples was presented in Table 1 according to X-ray fluorescence spectrometry (XRF) analysis.

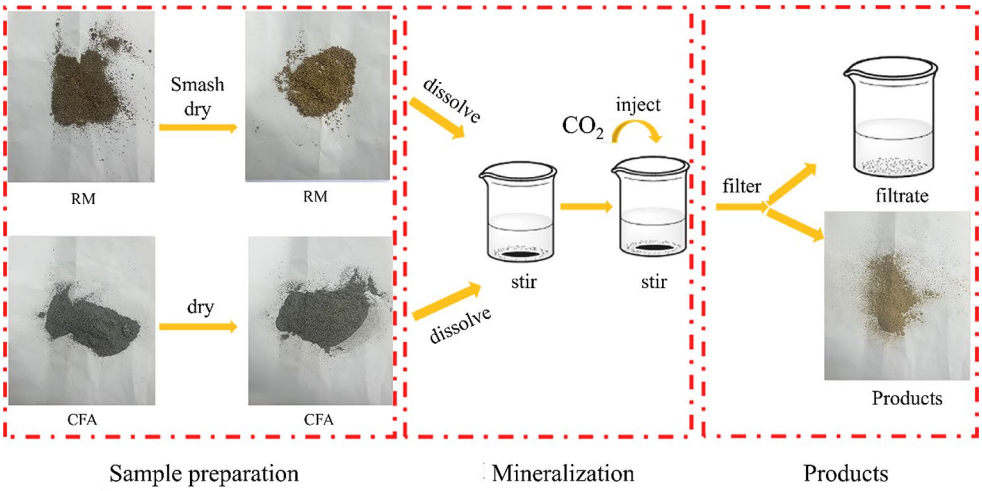

Fig. 1 Diagram representing the experimental procedure

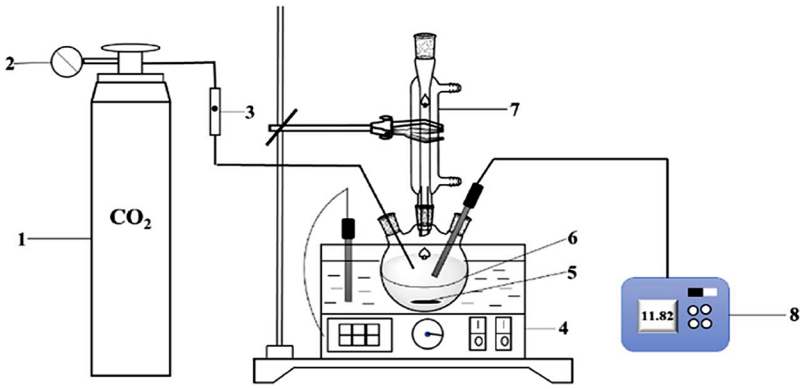

Fig. 2 Schematic diagram of the experimental apparatus

1−CO_2 cylinder; 2-pressure gauge; 3-gas flow meter; 4-water batch; 5-magnetic stirring; 6-reaction glass container; 7-condenser; 8-pH meter

2.2 Experimental section

The CO_2 mineralization process was conducted as follows. Initially, 100 mL of deionized water was added to a three-necked flask and placed on a thermostatic magnetic stirrer. The reactions were conducted at a specific temperature for a certain duration of time, with varying CO_2 flow rate and amount of reactants. The raw materials underwent a 5-minute hydrolysis in a three-necked flask. Subsequently, CO_2 was injected into the flask while continuously monitoring the pH value. CO_2 injection continued until the pH value remained stable for 10 min, upon which the reaction was terminated. Finally, the carbonated solid product was filtered, and the residue was dried at 105 °C for 4 h. The experimental process and equipment used are depicted in Figs. 1 and 2, respectively.

2.3 Sample characterization

Multiple analytical techniques were employed to investigate the mineralization behavior and product characteristics. The mineralization rate was determined in real-time using an online pH meter (PHS-201 F, China). The microstructure and elemental composition of the raw materials and mineralization products were observed using scanning electron microscopy and energy dispersive spectroscopy (SEM-EDS, HITACHI, S-4800, Japan). XRD (D2-Phaser, Bruker, Germany) was used to identify the mineralogy of the raw materials and mineralization products. The chemical composition of the raw materials was analyzed using X-ray fluorescence spectrometry (XRF, S8 Tiger, Bruker, Germany). The thermal stability of the raw materials and mineralization products was determined using thermogravimetric analysis (TG, Pyris 1, Perkinelmer, USA) with an Al_2O_3 crucible. The structural changes of the materials before and after mineralization were analyzed using Fourier transform infrared spectroscopy (FT-IR, Shimadzu IR Affinity-I). The infrared spectra of all samples were collected in the wavenumber range of 400–4000 cm^{-1} using the KBr pellet method.

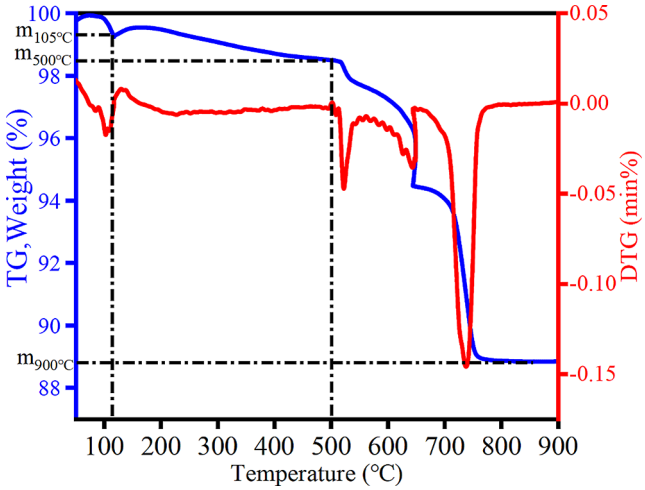

Fig. 3 TG-DTG curve of sample during carbonation reaction

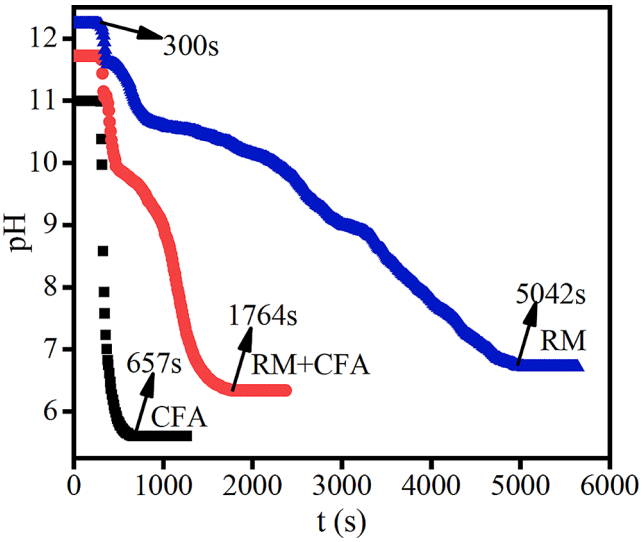

Fig. 4 t-pH curve of carbonation reaction for CFA, RM + CFA and RM.

2.4 Calculation of CO_2 mineralization efficiency and rate

The mineralization efficiency of the alkaline solid waste was calculated using Eqs. (1)-(3) (Vassilev and Vassileva 2020; Miao et al. 2021). The theoretical carbonation capacity of the solid waste was determined using Eq. (1):

$$Th_{\_m_{CO_2}} = \left[\frac{44}{56}\left(m_{CaO} + \frac{44}{40}m_{MgO} - \frac{56}{80} \times m_{SO_3}\right) + \frac{44}{40}m_{MgO} \times 1000\right] \quad (1)$$

where $Th_{\_m_{CO_2}}$ (g-CO_2/kg- solid waste) represents theoretical CO_2 storage mass fraction, while m_{CaO} (g-CaO/g-solid waste), m_{SO_3} (g-SO_3/g- solid waste), and m_{MgO} (g-MgO/g- solid waste) are the mass fractions of CaO, SO_3, and MgO in the sample, respectively.

The weight loss of the mineralization product obtained from the thermal gravimetric analysis (Fig. 3) indicated that the weight loss before 105 °C was due to the evaporation of free water in the product (Ji et al., 2019), while the weight loss between 105 and 500 °C was due to the loss of bound water in the product. The weight loss between 500 and 900 °C was attributed to the decomposition of calcium carbonate in the CFA, resulting in the release of CO_2 (Ni et al. 2017).

Equation (2) was used to determine the carbonation capacity of the sample (Wang 2019):

$$m_{CO_2} = \frac{\Delta m_{500-900°C}}{m_{105°C} - \Delta m_{500-900°C}} \times 1000 \quad (2)$$

where m_{CO_2} represents the carbonation capacity, $\Delta m_{500-900°C}$ is the weight of fixed CO_2 after reaction, and $m_{105°C} - \Delta m_{500-900°C}$ is the weight of the raw material. $\Delta m_{105°C}$ is the mass before the decomposition of the mineralization product.

The mineralization efficiency was defined using Eq. (3), The results obtained from the mineralization efficiency calculations were used to assess the potential of the alkaline solid waste as a CO_2 storage material:

$$\delta\,(\%) = \frac{m_{CO_2}}{Th_{-mCO_2}} \times 100\% \quad (3)$$

Equation (4) defines CO_2 mineralization rate, and the outcomes from these calculations could evaluate the speed at which the alkaline solid waste could be utilized as a CO_2 sequestration material (Ma et al. 2021).

$$\vartheta = \frac{pH_{final} - pH_{initial}}{t} \quad (4)$$

pH_{final} signifies the pH level at the end of CO_2 mineralization, $pH_{initial}$ denotes the pH level at the begin of CO_2 mineralization, while *t* denotes the duration of the mineralization reaction.

3 Results and discussion

3.1 Comparison of CO_2 mineralization in the single and composite systems

As displayed in Fig. 4, the initial pH of aqueous solution with dispersing CFA was approximately 11.0, which rapidly dropped to 5.6 at the end of the reaction. The dispersed RM-containing aqueous solution had a initial pH of 12.2, which underwent mineralization to achieve a pH of 6.7. For the

composite system of RM and CFA, the pH initially reached 11.7, which was due to OH^- concentration increase resulting from alkaline species hydrolysis in RM. The composite system exhibited a pH close to 6.3 at the end of the reaction, surpassing the pH of the single CFA system.

The mineralization equilibrium time for CFA, RM + CFA, and RM was found to be 357 s, 1464 s, and 4742 s, respectively. The expected mineralization equilibrium time (Δt) and mineralization rate of CFA + RM were calculated to be 2549.5 s ($\frac{357+4742}{2}$) and 0.0021 units/s ($\frac{5.4}{2549.5}$) (Ma et al. 2021), respectively. However, the actual Δt and mineralization rate of CFA+RM during the pH drop process were 1464 s and 0.0037 units/s ($\frac{5.4}{1464}$), respectively. The mineralization rate increased by 76.2% ($\frac{0.0037-0.0021}{0.0021} \times 100\%$). When the RM:CFA ratio was 1:1, the expected carbonation capacity should have been 120.35 (g-CO_2/kg-solid waste) ($\frac{237.2+3.5}{2}$) (Fig. 5) (Ni et al. 2017), while the actual carbonation capacity was 135.51 (g-CO_2/kg-solid waste). The carbonation capacity increased by 12.60% ($\frac{135.51-120.35}{120.35} \times 100\%$). These findings demonstrated the presence of a synergistic effect between RM and CFA, resulting in heightening mineralization rate, carbonation capacity, and mineralization efficiency.

The temperature and CO_2 flow rate were generally assumed to be the factors that impacted the mineralization reaction (He et al. 2013). As shown in Fig. 6a, the mineralization efficiency initially increased and then decreased with increasing temperature. The phenomenon could be attributed to the exothermic nature of the mineralization reaction, which was not conducive to the reaction at high temperatures (Lee et al., 2018). Additionally, excessively high temperatures could lead to decreasing the solubility of CO_2 in the aqueous solution. Furthermore, increasing CO_2 flow rate resulted in the stabilization of mineralization efficiency, as exhibited in Fig. 6b. This observation could be explained by the low solubility of CO_2 in water, i.e., a small amount of CO_2 could saturate the aqueous solution, making the effect of CO_2 flow rate not obvious.

3.2 Influence of different CFA:RM ratios in the composite system on CO_2 mineralization

The carbonation capacity of the sample at an RM:CFA ratio of 5:5 was expected to be 120.35 g-CO_2/kg-solid waste based on calculations. However, the actual carbonation capacity was found to be 135.51 g-CO_2/kg-solid waste, indicating a 12.60% increase in carbonation capacity. This fact highlighted the synergistic effect of RM and CFA on CO_2 mineralization.

Figure 7 illustrates the changes in mineralization capacity and efficiency of RM and CFA at various ratios. The mineralization capacity of the composite obviously decreased as

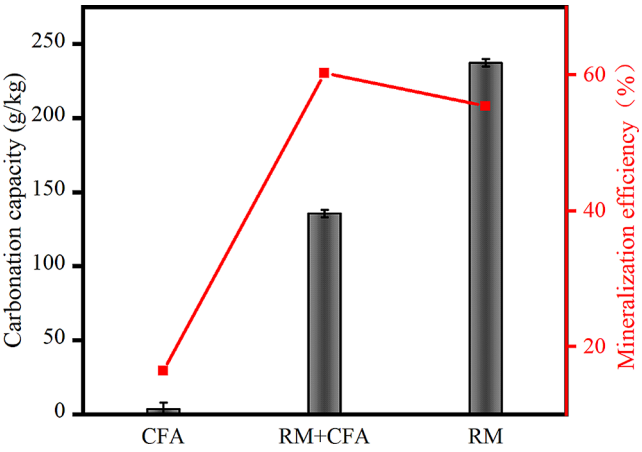

Fig. 5 Performance of CFA, RM + CFA and RM in carbonation reaction

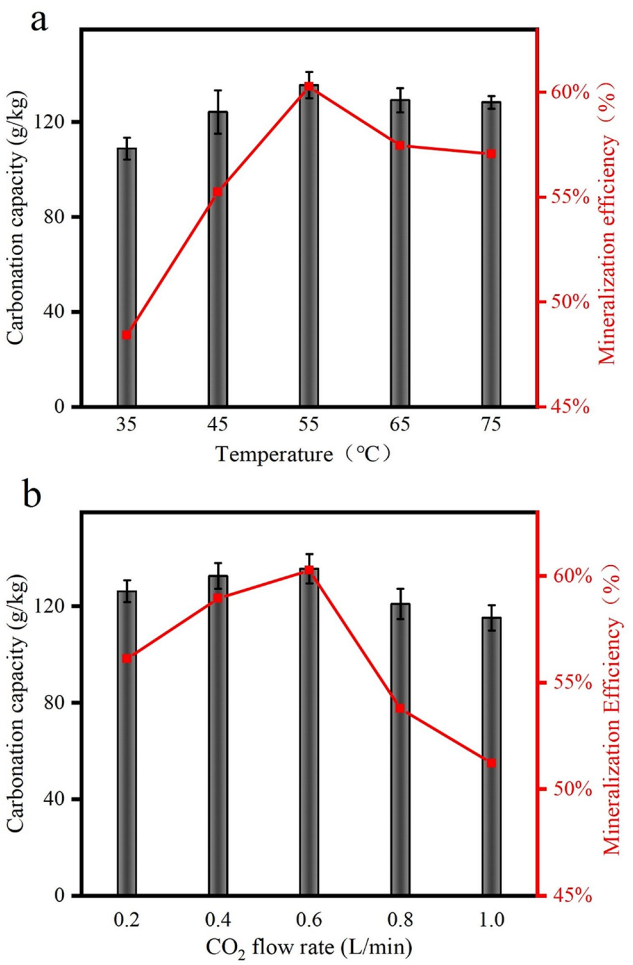

Fig. 6 **a** Effects of temperature and **b** CO_2 flow rate on CO_2 mineralization

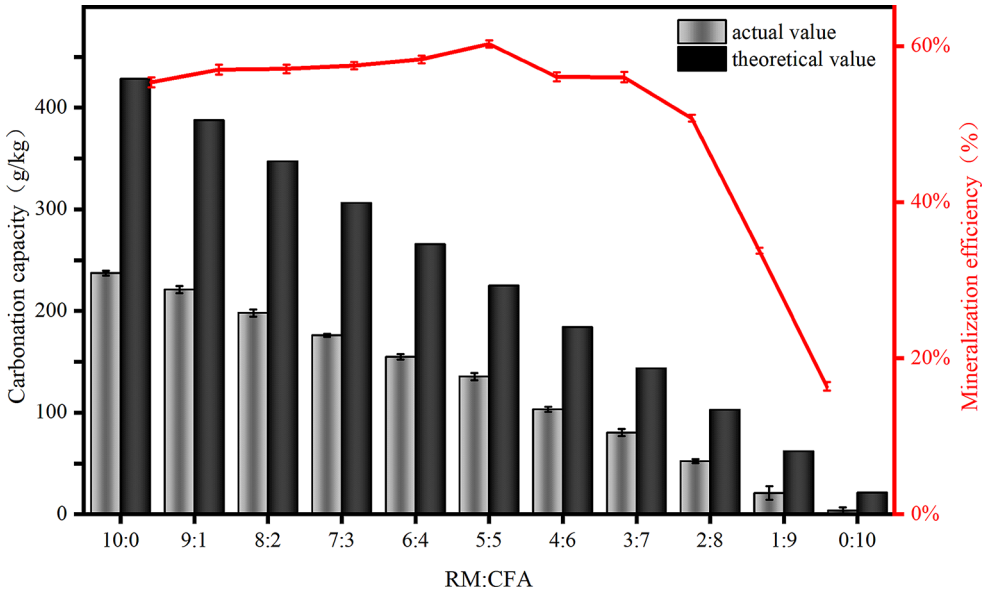

Fig. 7 Performance for CO_2 mineralization in the composite of CFA and RM with different ratio

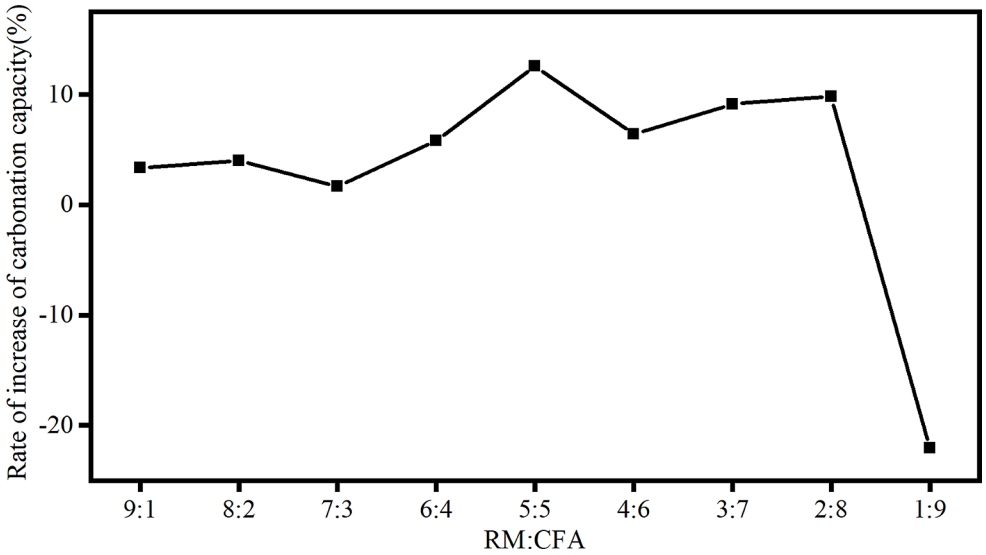

Fig. 8 Rate variation of carbonation capacity for the composite of CFA and RM with different ratio

the ratio of RM and CFA reduced. The mineralization efficiency gradually increased when the ratio of RM and CFA ranged from 10:0 to 5:5, and it decreased when the ratio of RM was less than 5:5. These results provided compelling evidence of the enhanced mineralization reaction resulting from the synergistic effect of RM and CFA. Interestingly, a gradual decrease in RM content within the composite system was correspond to a gradual decrease in the theoretical carbonation capacity. However, contrary to expectations, the mineralization efficiency demonstrated a gradual increase until the RM to CFA ratio reached 5:5. Remarkably, the maximum mineralization efficiency was achieved at this specific ratio.

Figure 8 illustrates the growth rate of carbonation capacity under different RM and CFA ratios. A negative growth rate of -22.91% was observed at the 1:9 of RM and CFA ratio, indicating a negative synergistic effect on mineralization. In contrast, positive growth rates were all observed for other ratios, signifying a synergistic effect under those conditions. Notably, the highest growth rate of carbonation capacity, reaching 12.60%, was achieved at the 5:5 RM:CFA ratio. These findings further confirmed the synergistic effect of RM and CFA on CO_2 mineralization, and underscored the critical role of an optimized RM and CFA ratio in maximizing mineralization efficiency.

3.3 Insight into of synergistic effect in the composite system for CO_2 mineralization

The cooperative impact of CFA and RM composite systems on CO_2 mineralization was examined by analyzing

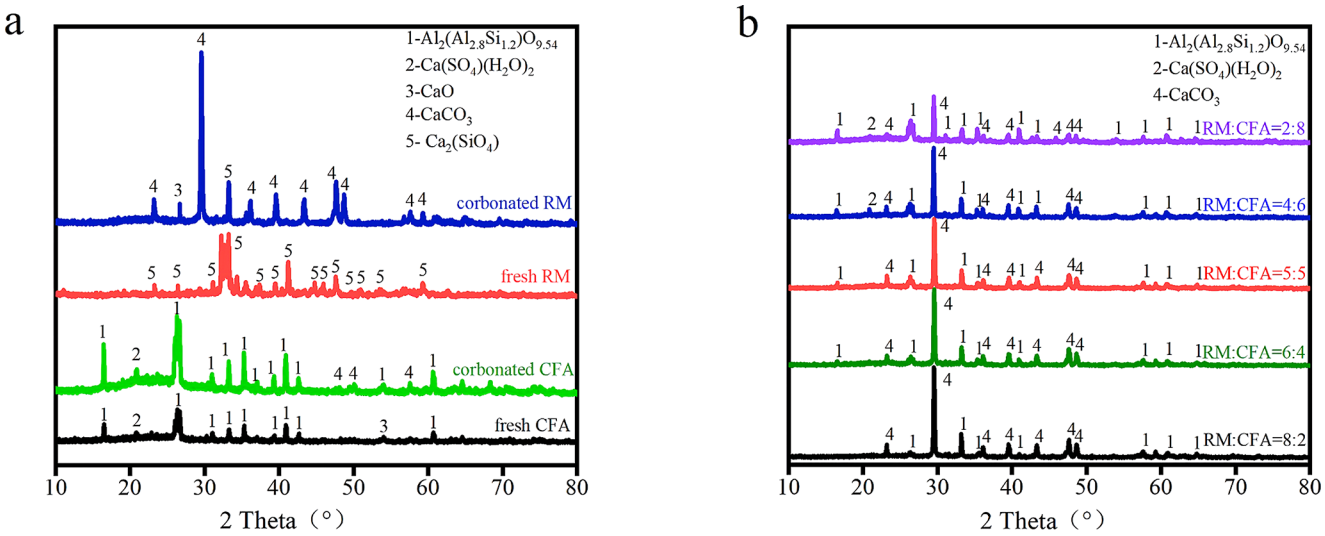

Fig. 9 XRD patterns of **a** fresh and carbonated CFA and RM and **b** carbonated the composite of CFA and RM

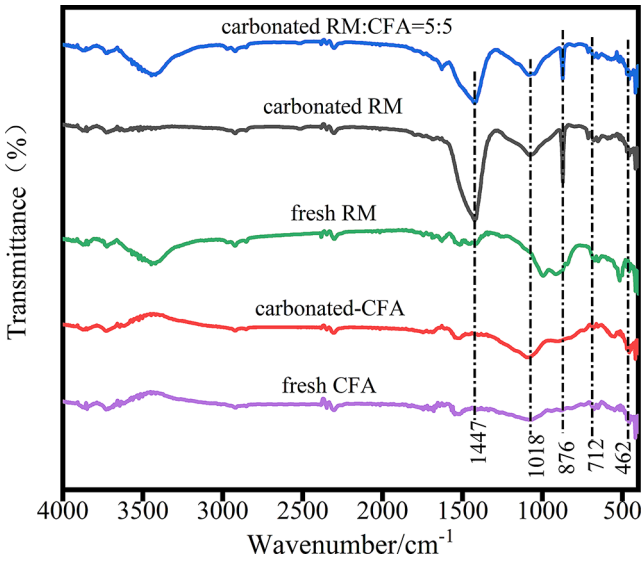

Fig. 10 FT-IR spectra of fresh materials and carbonated products

the mineralogical features of these composite systems before and after mineralization. As depicted in Fig. 9, the peaks corresponding to CaO and $Ca(SO_4)(H_2O)_2$ were observed by referencing standard PDF cards during XRD analysis, which was in accordance with the report (Ji et al., 2019). The existence of inactive $Ca(SO_4)(H_2O)_2$ could account for the low mineralization efficiency observed in CFA. The high reactivity of $2CaO{\cdot}SiO_2$ (C2S) in raw RM resulted in a substantial production of $CaCO_3$. In the composite system, the inclusion of RM resulted in the disappearance of the peak associated with $Ca(SO_4)(H_2O)_2$ after mineralization when the RM:CFA ratio exceeded 5:5. However, if the RM:CFA ratio was less than 5:5, the $Ca(SO_4)(H_2O)_2$ peak persisted, indicating that the alkalinity supplied by RM may not fully dissolve $Ca(SO_4)(H_2O)_2$, potentially accounting for the reduced mineralization efficiency at RM:CFA ratios below 5:5. Upon surpassing a 5:5 ratio of RM to CFA, the inactive $Ca(SO_4)(H_2O)_2$ of CFA could be fully dissolved in the composite system, which would lead to a sharp Ca^{2+} increase and the corresponding calcium carbonate. The produced calcium carbonate would cover the surface of RM besides CFA, which would hinder further releasing of other Ca^{2+} in the interior part of RM, thus leading to mineralization efficiency decrease.

As shown in Fig. 10, all five samples displayed peaks at 712 cm^{-1}, indicating the presence of $CaCO_3$. Furthermore, peaks at 876 cm^{-1} and 1447 cm^{-1} were observed in carbonated RM: CFA of 5:5, carbonated CFA, and carbonated RM, which were assigned to the out-of-plane bending vibrations and anti-symmetric stretching vibration of the C-O group in $CaCO_3$, respectively. According to the previous literature (Wang 2019), these peaks corresponded to the in-plane and out-of-plane bending vibrations of the O-CO- group in $CaCO_3$, respectively.

SEM observations were carried out on the provided raw materials and mineralized products, as depicted in Fig. 11. After CO_2 mineralization in the single RM system, numberous fine needle-shaped calcium carbonate crystals were covered on RM surface, limiting further releasing of Ca^{2+} in the internal RM. Conversely, a small quantity of flake-like calcium carbonate was attached on CFA surface due to its low Ca^{2+} releasing in the single CFA system. Within the composite system, substantial Ca^{2+} was released from calcium species, leading to large amount of calcium carbonate formation. The generated calcium carbonate not just covert the RM surface but also attached to CFA surface. Reduced calcium carbonate coverage on RM surface was expected to enhance further

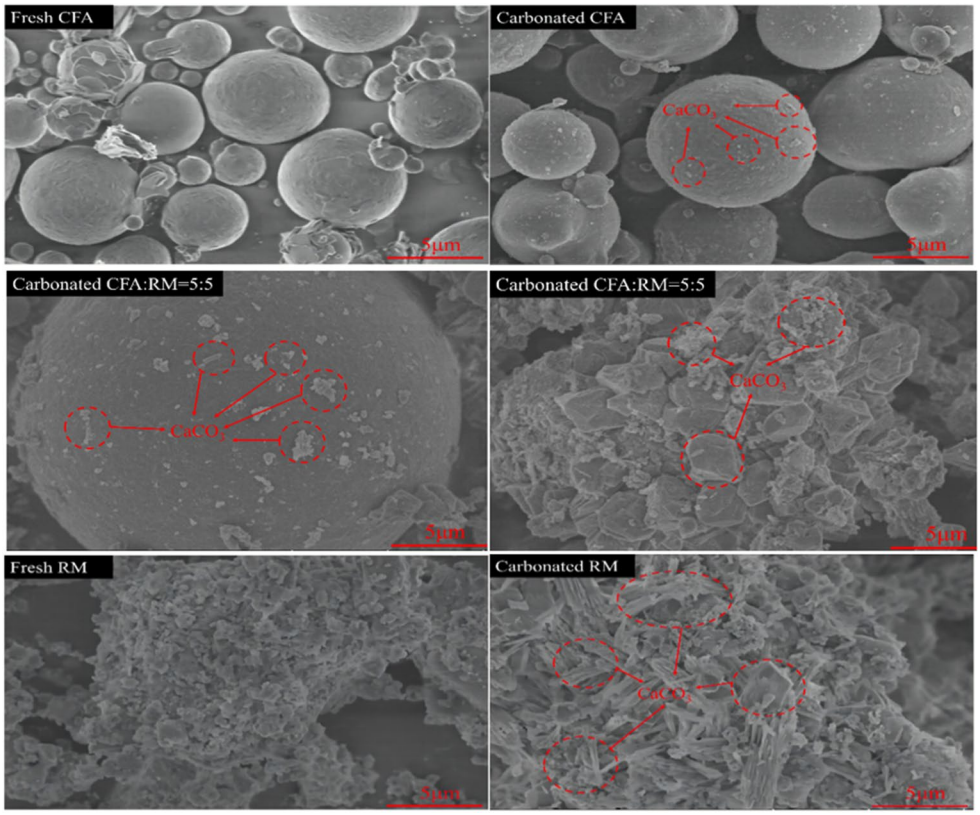

Fig. 11 SEM images of fresh materials and carbonated products

releasing of Ca^{2+} in the internal RM, thus facilitating CO_2 mineralization in the composite system.

The synergistic effect of CFA and RM accelerated the efficiency and rate of CO_2 mineralization. In the composite system, CFA offered large amounts of surface attachment sites for the generated calcium carbonate, which would reduce the coverage of calcium carbonate on the RM surface, facilitating the releasing of Ca^{2+} in RM. Furthermore, alkaline oxides in RM underwent hydrolysis in the composite system, releasing high concentrations of OH^-. The increased alkalinity encouraged the dissolution of $Ca(SO_4)(H_2O)_2$ within the CFA, increasing the free Ca^{2+} in the composite system, thereby elevating the CO_2 mineralization efficiency. Additionally, the increased alkalinity with the inflution of RM promoted CO_2 mineralization rate (Song et al. 2020).

4 Conclusions

In this study, the effect was investigated for combining CFA and RM for CO_2 mineralization, which revealed that the combined system of CFA and RM had a positive impact on the mineralization rate and efficiency. Notably, the mineralization rate and efficiency increased by 76.2% and 12.60% in a composite system of CFA and RM with mass ration of 5:5, respectively, compared to the calculated weighted averaged ones in the individual CFA and RM. The synergistic effect of RM and CFA was attributed to the ectopic adherence of the generated calcium carbonate to CFA surface and the increased alkalinity of the system caused by RM addition. The ectopic adherence of calcium carbonate to CFA surface promoted Ca^{2+} releasing from the internal RM. Moreover, the increased alkalinity leaded to the dissolution of the inactive $CaSO_4(H_2O)_2$ in CFA. This study would provide valuable insights into the synergistic effects of different components on CO_2 mineralization and pave the way for the development of effective and efficient CO_2 mineralization.

Acknowledgements This work was financially supported by National Natural Science Foundation of China (21706172); Shanxi Province Natural Science Foundation (202203021221069 and 20210302123167).

Author contributions Zhenchao Yao Data curation, Writing the original manuscript. Yugao Wang Project administration, Supervision, Providing funding acquisition and resources, Reviewing and Editing. Jun Shen Reviewing and Editing, Providing funding acquisitionand resources. Yanxia Niu Reviewing and Editing. Jiangfeng Yang Project administration, Proofreading, and Editing. Xianyong Wei Reviewing and Editing.

Declarations

Declaration of competing interest The authors declare that they have no known competing financial interests or personal relationships that could have appeared to influence the work reported in this paper.

References

Afra S, Alhosani M, Firoozabadi A (2023) Improvement in CO_2 geo-sequestration in saline aquifers by viscosification: from molecular scale to core scale. INT J GREENH GAS CON 125:103888–103889

Bajracharya S, Srikanth S, Mohanakrishna G, Zacharia R, Strik DP, Pant D (2017) Biotransformation of carbon dioxide in bioelectrochemical systems: state of the art and future prospects. J Power Sources 356:256–273

Brent GF, Allen DJ, Eichler BR, Petrie JG, Mann JP, Haynes BS (2012) Mineral carbonation as the core of an industrial symbiosis for energy-intensive minerals conversion. J Ind Ecol 16:94–104

Dananjayan RRT, Kandasamy P, Andimuthu R (2016) Direct mineral carbonation of coal fly ash for CO_2 sequestration. J Clean Prod 112:4173–4182

Ding Lu, Yang Mingming, Dong Kai, N. Vo Dai-Viet, Hungwe Douglas, Ye Jiahan, Ryzhkov Alexander, Yoshikawa Kunio (2022) Mobile power generation system based on biomass gasification. Int J Coal Sci Technol 9(1):34. https://doi.org/10.1007/s40789-022-00505-0

Fernández, González J, Rumayor M, Domínguez-Ramos A, Irabien Á (2022) CO_2 electroreduction: sustainability analysis of the renewable synthetic natural gas. INT J GREENH GAS CON 114:103549–103556

Genç-Fuhrman H, Tjell JC, McConchie D (2004) Adsorption of arsenic from water using activated neutralized red mud. Environ Sci Technol 38:2428–2434

Han YS, Ji S, Lee PK, Oh C (2017) Bauxite residue neutralization with simultaneous mineral carbonation using atmospheric CO_2. J Hazard Mater 326:87–93

He L, Yu D, Lv W, Wu J, Xu M (2013) A Novel Method for CO_2 sequestration via Indirect Carbonation of coal fly Ash. Ind Eng Chem Res 52:15138–15145

Ho HJ, Iizuka A, Shibata E (2021) Utilization of low-calcium fly ash via direct aqueous carbonation with a low-energy input: determination of carbonation reaction and evaluation of the potential for CO_2 sequestration and utilization. J Environ Manage 288:112411–112415

Ji L, Yu H, Wang X, Grigore M, French D, Gözükara YM, Yu J, Zeng M (2017) CO_2 sequestration by direct mineralization using fly ash from Chinese Shenfu coal. Fuel Process Technol 156:429–437

Koytsoumpa EI, Bergins C, Kakaras E (2018) The CO_2 economy: review of CO_2 capture and reuse technologies. J Supercrit Fluids 132:3–16

Lee KG, Bae SJ (2018) Carbonation of circulating fluidized Bed Combustion fly Ash with Hybrid reaction. J Korean Ceram Soc 55:160–165

Liang G, Chen W, Nguyen AV, Nguyen TA (2018) Red mud carbonation using carbon dioxide: effects of carbonate and calcium ions on goethite surface properties and settling. J Colloid Interface Sci 517:230–238

Liu W, Su S, Xu K, Chen Q, Xu J, Sun Z, Wang Y, Hu S, Wang X, Xue Y, Xiang J (2018) CO_2 sequestration by direct gas-solid carbonation of fly ash with steam addition. J Clean Prod 178:98–107

Ma Z, Liao H, Cheng F (2021) Synergistic mechanisms of steelmaking slag coupled with carbide slag for CO_2 mineralization - ScienceDirect. INT J GREENH GAS CON 105:103229–103230

Miao ED, Du Y, Wang HY, Xiong Z, Zhao YC, Zhang JY (2021) Experimental study and kinetics on CO_2 mineral sequestration by the direct aqueous carbonation of pepper stalk ash. Fuel 303:121230–121237

Mucsi G, Halyag N, Kurusta T, Kristaly F (2021) Control of Carbon Dioxide Sequestration by Mechanical activation of Red Mud. Waste Biomass Valorization 12:6481–6495

Ni P, Xiong Z, Tian C, Li H, Zhao Y, Zhang J, Zheng C (2017) Influence of carbonation under oxy-fuel combustion flue gas on the leachability of heavy metals in MSWI fly ash. Waste Manage 67:171–180

Noack CW, Dzombak DA, Nakles DV, Hawthorne SB, Heebink LV, Dando N, Gershenzon M, Ghosh RS (2014) Comparison of alkaline industrial wastes for aqueous mineral carbon sequestration through a parallel reactivity study. Waste Manage 34:1815–1822

Pei SL, Pan SY, Li YM, Chiang P-C (2017) Environmental Benefit Assessment for the Carbonation process of Petroleum Coke fly Ash in a Rotating Packed Bed. Environ Sci Technol 51:10674–10681

Ram AK, Mohanty S (2022) State of the art review on physiochemical and engineering characteristics of fly ash and its applications. Int J Coal Sci Technol 9(1):9. https://doi.org/10.1007/s40789-022-00472-6

Revathy TDR, Ramachandran A, Palanivelu K (2021) Sequestration of CO_2 by red mud with flue gas using response surface methodology. Carbon Manag 12:139–151

Romanov V, Soong Y, Carney C, Rush GE, Nielsen B, O'Connor W (2015) Mineralization of carbon dioxide: a literature review. ChemBioEng Rev 2:231–256

Sanna A, Hall MR, Maroto, Valer M (2012) Post-processing pathways in carbon capture and storage by mineral carbonation (CCSM) towards the introduction of carbon neutral materials. Energy Environ Sci 5:7781–7796

Seifritz W (1990) CO_2 disposal by means of silicates. Nature. 486–486

Song W, Zhu Z, Pu S, Wan Y, Huo W, Song S, Zhang J, Yao K, Hu L (2020) Efficient use of steel slag in alkali-activated fly ash-steel slag-ground granulated blast furnace slag ternary blends. Constr Build Mater 259:119814–119827

Tsakiridis PE, Agatzini, Leonardou S, Oustadakis P (2004) Red mud addition in the raw meal for the production of Portland cement clinker. J Hazard Mater 116:103–110

Vassilev SV, Vassileva CG (2020) Extra CO_2 capture and storage by carbonation of biomass ashes. Energy Convers Manag 204:112331–112337

Wang Y (2019) Changes in mineral composition, growth of calcite crystal, and promotion of physico-chemical properties induced by carbonation of beta-C_2S. J CO_2 Util 34:149–162

Wang X, Maroto, Valer MM (2011) Dissolution of serpentine using recyclable ammonium salts for CO_2 mineral carbonation. Fuel 90:1229–1237

Wang B, Pan Z, Cheng H, Guan Y, Zhang Z, Cheng F (2020) CO_2 sequestration: high conversion of gypsum into $CaCO_3$ by ultrasonic carbonation. Environ Chem Lett 18:1369–1377

Yang J, Xiao B (2008) Development of unsintered construction materials from red mud wastes produced in the sintering alumina process. Constr Build Mater 22:2299–2307

Yao ZT, Ji X, Sarker P, Tang J, Ge L, Xia M, Xi Y (2015) A comprehensive review on the applications of coal fly ash. Earth-Sci Rev 141:105–121

Yuan Q, Yang G, Zhang Y, Wang T, Wang J, Romero CE (2022) Supercritical CO_2 coupled with mechanical force to enhance carbonation of fly ash and heavy metal solidification. Fuel 315:123154–123156

Zevenhoven R, Teir S, Eloneva S (2008) Heat optimisation of a staged gas–solid mineral carbonation process for long-term CO_2 storage. Energy 33:362–370